analytical chemistry

Article

pubs.acs.org/ac

Target-Triggered Enzyme-Free Amplification Strategy for Sensitive Detection of MicroRNA in Tumor Cells and Tissues

Yuhui Liao, Ru Huang, Zhaokui Ma, Yunxia Wu, Xiaoming Zhou,* and Da Xing*

MOE Key Laboratory of Laser Life Science & Institute of Laser Life Science, College of Biophotonics, South China Normal University, Guangzhou, China

ABSTRACT: MicroRNAs (miRNAs) participate in important processes of life course. Because of their characters of small sizes, vulnerable degradabilities, and sequences similarities, the existing detection technologies mostly contain enzymatic amplification reactions for acquisition of high sensitivities and specificities. However, specific reaction conditions and time-dependent enzyme activities are caused by the accession of enzymes. Herein, we designed a target-triggered enzyme-free amplification platform that is realized by circulatory interactions of two hairpin probes and the integrated electrochemiluminescence (ECL) signal giving-out component. Benefiting from outstanding performances of the enzyme-free amplification system and ECL, this strategy is provided with a simplified reaction process, high sensitivity, and operation under isothermal conditions. Through detection of the miRNA standard substance, the sensitivity of this platform reached 10 fmol, and a splendid specificity was achieved. We also analyzed three tumor cell lines (human lung adenocarcinoma, breast adenocarcinoma, and hepatocellular liver carcinoma cell lines) through this platform. The sensitivities of 10^3 cells, 10^4 cells, and 10^4 cells were, respectively, achieved. Furthermore, clinical tumor samples were tested, and 21 of 30 experimental samples gave out positive signals. Thus, this platform possesses potentials to be an innovation in miRNA detection methodology.

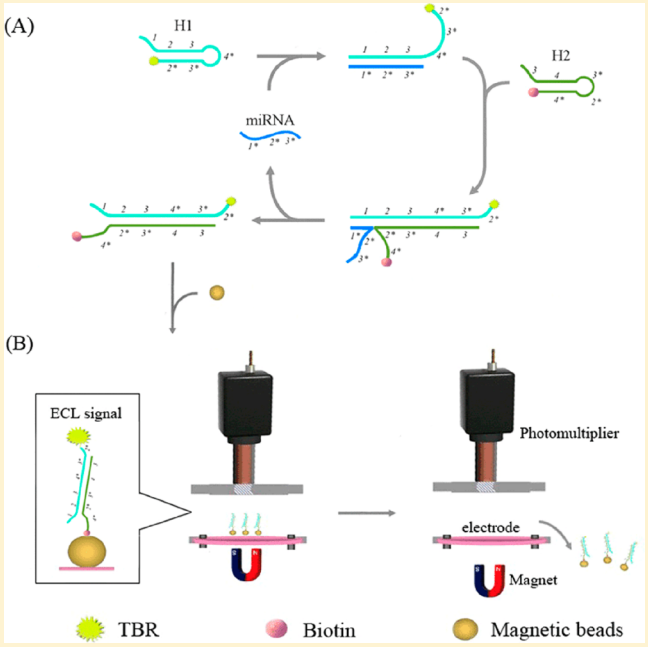

MicroRNAs (miRNAs) are highly conserved small single-stranded RNAs with the length of 18−25 nt,[1−4] encoded by noncoding endogenous genes.[5−7] Their functional mechanism in regulation of gene expression has attracted enormous attention, since the first miRNA was reported in the early 1990s.[8] To date, researchers have revealed that miRNAs participate in a large number of significant cell activities, including early development, cell proliferation, and apoptosis.[9,10] Moreover, their expression levels are directly related to many kinds of cancers, could reflect the gene-like actions of the oncogene or the tumor suppressor.[11−14] Therefore, miRNAs can be used as valuable biomarkers for cellular level research and related diseases, and their qualification possesses great significance in the clinical applications of tumor molecular diagnosis.

However, quantitative detection of miRNAs has always been a tough call that is attributed to their small size, vulnerable degradability, similarities of the sequences, and relatively low expression levels in cells. Conventional methods, such as Northern blot,[15−17] are obsessed with low sensitivity, time, and labor consumption. Reverse transcriptase PCR (RT-PCR) and its derivatives,[18−20] real-time reverse transcriptase PCR (real-time RT-PCR),[21−23] are playing an increasingly important role in routine tests with high sensitivity and specificity. However, the miRNA detection methodology needs a diversified means response to different requirements. As the supplement of miRNA detection methodology, microarray technology provides a novel approach to miRNA detection that could process a large number of miRNA samples in a short time and make multiplex detection possible.[24,25] However, the low sensitivity impedes the promotion and popularization of the microarray. In recent years, the DNA-based detection assay shows excellent performance and great reference significance in microRNA detection.[26−29]

For acquisitions of high sensitivities and preferable specificities, the existing detection technologies mostly contain an enzymatic amplification system. However, the characteristics of enzymes such as specific reaction conditions, the reaction-time dependent enzyme activity, and difficulties in storage are caused by the accession of enzyme. Therefore, enzyme-free

Received: February 25, 2014
Accepted: April 2, 2014
Published: April 2, 2014

   dx.doi.org/10.1021/ac5007427 | *Anal. Chem.* 2014, 86, 4596−4604

Table 1. Sequences of Hairpin Probes and MicroRNAs

note	sequences (5′ → 3′)					
microRNA-21	UAG CUU AUC AGA CUG AUG UUG A					
microRNA-210	CUG UGC GUG UGA CAG CGG CUG A					
microRNA-214	ACA GCA GGC ACA GAC AGG CAG U					
H1	1	2	3	4*	3*	2*
(3′Amino)	TCAACATC	AGTCTGA	TAAGCTA	CCATGTGTAGA	TAGCTTA	TCAGACT
H2	3	4	3*	2*	4*	
(3′Biotin)	TAAGCTA	TCTACACATGG	TAGCTTA	TCAGACT	CCATGTGTAGA	

amplification methods possess incomparable advantages relative to enzymatic amplification except for the weakened amplification efficiencies. Thus, an efficient pattern of enzyme-free amplification or an integrated signal giving-out system with high efficiencies should produce positive effects. Serving as the indispensable signal giving-out system of immune diagnosis methodology, electrochemiluminescence (ECL) has achieved revolutionary progress in molecular diagnosis technologies.[30−32] Because of its wide detection range, controlled reaction system, short time consumption, and high sensitivity and signal-to-noise ratio, ECL has gained enormous interest in detection methodology[33−35] since the first detailed ECL issue was published in the 1960s.[36] In this paper, ECL is integrated as the signal giving-out component that lays out the foundation of high sensitivity and signal-to-noise ratio and provides a rapid detection mode with a wide detection range.

Herein, we construct a target-triggered enzyme-free amplification platform realized by the circulatory interaction of two hairpin probes, which is inspired by programming biomolecular self-assembly pathways.[37−40] It overcomes the disadvantages of enzymatic amplification. In the whole process, no enzymes are involved. Thus, the reactive conditions are greatly simplified. This strategy is provided with a simple reaction process that operates under isothermal conditions in phosphate buffered saline. The sequence-specific probes are newly designed, and high sensitivity and specificity are achieved. Through detection of the miRNA standard substance, as low as 10 fmol of miRNA21 can be detected by this platform. We also analyzed three tumor cell lines (human lung adenocarcinoma, breast adenocarcinoma, and hepatocellular liver carcinoma cell lines) through this platform. The sensitivities of 10^3 cells, 10^4 cells, and 10^4 cells were, respectively, achieved. Furthermore, clinical tumor samples were tested, and 21 of 30 experimental samples gave the positive signals. Thus, this platform provides excellent performance in miRNA detection and possesses the potential to be an innovation of tumor molecular diagnosis.

EXPERIMENTAL SECTION

Reagents. Streptavidin magnetic beads were obtained from New England BioLabs. DEPC-treated water and RNAase inhibitor were the products of Takara Biotechnology (Dalian) Co., Ltd. Phosphate buffered saline (PBS) buffer (20×) solution and the regents related to electrophoresis were purchased from Shanghai Sangon Biotechnology Co. Ltd. SYBR I and SYBR II were purchased from Invitrogen. All chemicals used were of reagent-grade and were purchased from Sigma-Aldrich and used without further purification except where noted. All oligonucleotides and probes synthesized in this work were purified by Invitrogen. ECL signal were recorded by Elecsys2010 system. All the consumable items were treated by DEPC and sterilized three times.

Preparation of Probes. Through this approach, miRNA21 was chosen as the ideal analyte. For the purpose of establishing the miRNA detection platform, hairpin probe 1 (H1) and hairpin probe 2 (H2) were designed based on the principle of the enzyme-free amplification system. In addition, the miRNA21's sequence was taken into account. The sequence and modification of H1 and H2 are listed in Table 1. H1 are tagged with Ru $(bpy)_3^{2+}$-NHS, and H2 are labeled with biotin. Before the construction of enzyme-free amplification system, both H1 and H2 were treated in a process of gradient cooling treatment. The process contained a fully denaturation at 95 °C for 5 min and a gradient cooling step that drop 5 degrees per minute until cooling down to the room temperature. Then the probes are stored at 4 °C for later use.

Total RNA Extration from Cell Lysates and Tumor Tissues Samples. MiRNAs were extracted from three cell lysates, human lung adenocarcinoma cells (A549), human breast adenocarcinoma cells (MCF-7), human hepatocellular liver carcinoma cells (HepG2), and the corresponding tumor tissue, by using a commercial total-RNA extracting kit. Normal human liver cells (LO2), normal skin cells (HUVEC), and normal human bronchial epithelial cell line (HBE) were chosen as the normal miRNA expression level control. Before extraction, the clinical tumor tissues are pretreated with liquid nitrogen and ground into a paste, followed by small RNA extraction by a commercial kit. The tumor cell lines are processed with cell counting before extraction.

Polyacrylamide Gel Electrophoresis. To verify the feasibility of enzyme-free amplification system, the amplified products were analyzed on a Biorad slab electrophoresis system (Bio-Rad Laboratories). A 10% native polyacrylamide gel (29:1 acrylamide: bis-acrylamide) loaded with 10 μL samples was run at room temperature for 45 min at 120 V, in 1 × Tris-borate-EDTA (TBE), then followed the coloration of SYBR I and SYBR II and photographing of Biorad Digital imaging system.

Construction of Enzyme-Free Amplification Platform. The enzyme-free amplification system consists of hairpin probes (H1 and H2), PBS buffer, RNAase inhibitor, and DEPC-treated water. The final reaction volume is set as 100 μL. The final concentration of H1 and H2 are all set as 50 nM. PBS buffer concentration is determined as 0.8×. The RNAase inhibitor reached a final concentration of 1 U/μL.

The whole platform consists of an enzyme-free amplification system and an ECL signal giving-out system. The whole operation procedures were conducted with the following steps: enzyme-free amplification, magnetic beads capturing and cleaning process, and ECL signal detection. Then the miRNA21 exists, and enzyme-free amplification system were initiated. After 1 h of amplification, the products are captured by streptavidin magnetic beads for 30 min at 38 °C. Then with the separation of the magnetic separator, the complexes of amplification products and streptavidin magnetic beads were

dx.doi.org/10.1021/ac5007427 | Anal. Chem. 2014, 86, 4596−4604

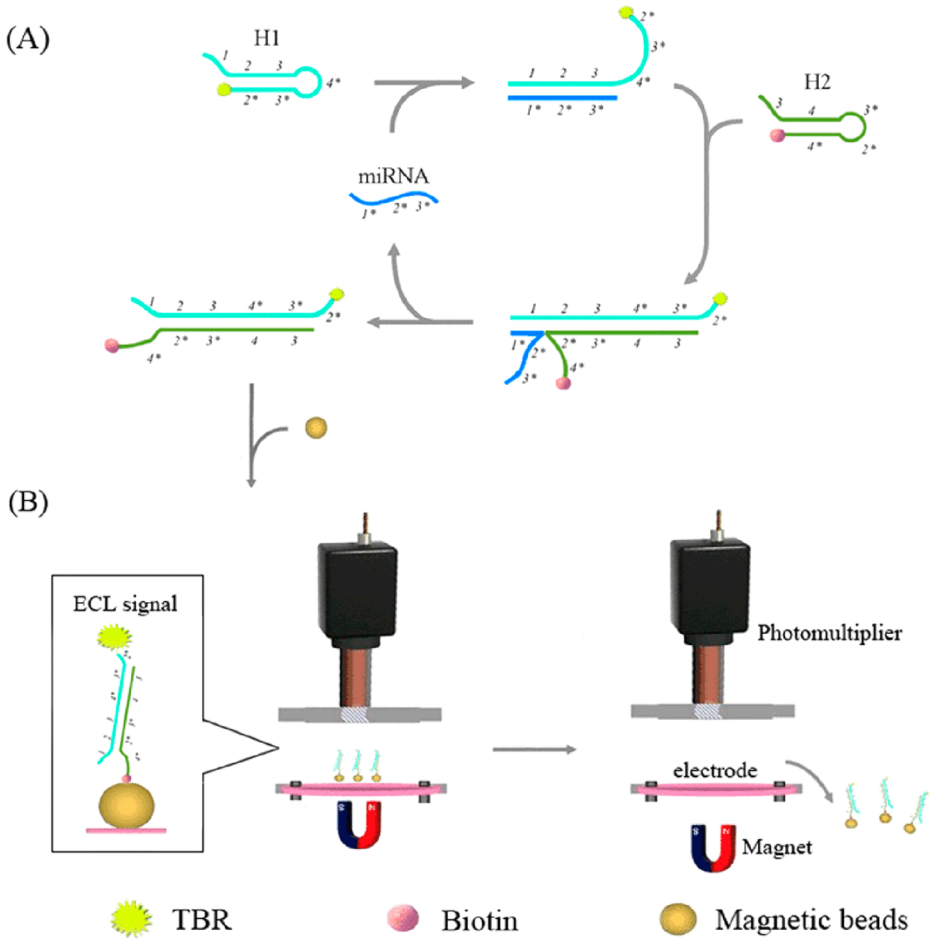

Figure 1. Principle of the enzyme-free miRNA detection platform: (A) principle of enzyme-free amplification system and (B) ECL signal giving-out steps.

redissolved in 1× PBS buffer. After the cleaning process was repeated three times, the ECL signals are detected by the Elecsys2010 system.

RESULTS AND DISCUSSION

Design of the MiRNA Detection Platform. This approach aims at the construction of an enzyme-free miRNAs detection platform, which consists of the enzyme-free amplification and ECL signal giving-out steps. The overall concept of this strategy is shown in Figure 1. H1 and H2 are first treated with gradient cooling processes for the obtainment of complete hairpin structures. When target miRNA exists, the stem of H1 will be unfolded. As the result of H1's unfoldment, the hidden sequence of H1's stem is exposed. It makes the unfoldment of H2 possible. Then with the interaction of H1 and H2, target miRNAs are released back to the enzyme-free amplification. It causes a new start of the circuit and the formation of H1−H2 complexes. After 1 h of amplification, H1−H2 complexes are captured by streptavidin magnetic beads and processed with magnetic separation and washing in PBS buffer. Finally, ECL signals related to target miRNAs are finally generated.

Probe Design Strategy and Validity of the Enzyme-Free Amplification System. As shown in Figure 1, H1 contains six domains termed as 1, 2, 3, 4*, 3*, 2*. The regions 1, 2, 3 are identification zones that are completely complementary with the target. Region 1 provides the breakthrough for unfoldment of H1, region 2 and 3 are necessary zones for formation of H1 hairpin structure. H2 contains five domains termed as 3, 4, 3*, 2*, 4*. The region 3, 4, 3*, 2* are complementary to H1. Region 3 provides the breakthrough for unfoldment of H2 while H1 are unfolded by target miRNA. Through the hybridization interaction of H1 and H2, target miRNA is displaced by region 3*, 2* of H2. Thus, target miRNA is released into the next circulation. For avoiding unnecessary false positive signal, H1 and H2 cannot interact with each other until the specific target is introduced. Hence, both of H1 and H2 must possess high melting temperature for unabridged formation of the hairpin structure. In this paper, the annealing temperature of H1 is 63.7 °C, and H2's is 62.9 °C (calculated by Oligo Analyzer 3.1). They are much higher than the reaction temperature, 38 °C.

The length of region 1 (H1) should meet both the H1 stability and target miRNA circulation efficiency. The length of regions 1, 2, 3 are invariable while the target miRNA are designated. Thus, longer region 1 leads to shorter regions 2 and 3 that is adverse for H1 stability. At the same time, the miRNA circulation is greatly suppressed because of enhanced affinity between region 1 and target miRNA that obstructs target miRNA released from H1−H2 complex. Herein, we set the length of region 1 as 8 nt on the basis of H1 stability. The annealing temperature of region 1 is 14.5 °C that is lower than the reaction temperature. The target miRNA circulation efficiency is guaranteed.

dx.doi.org/10.1021/ac5007427 | Anal. Chem. 2014, 86, 4596−4604

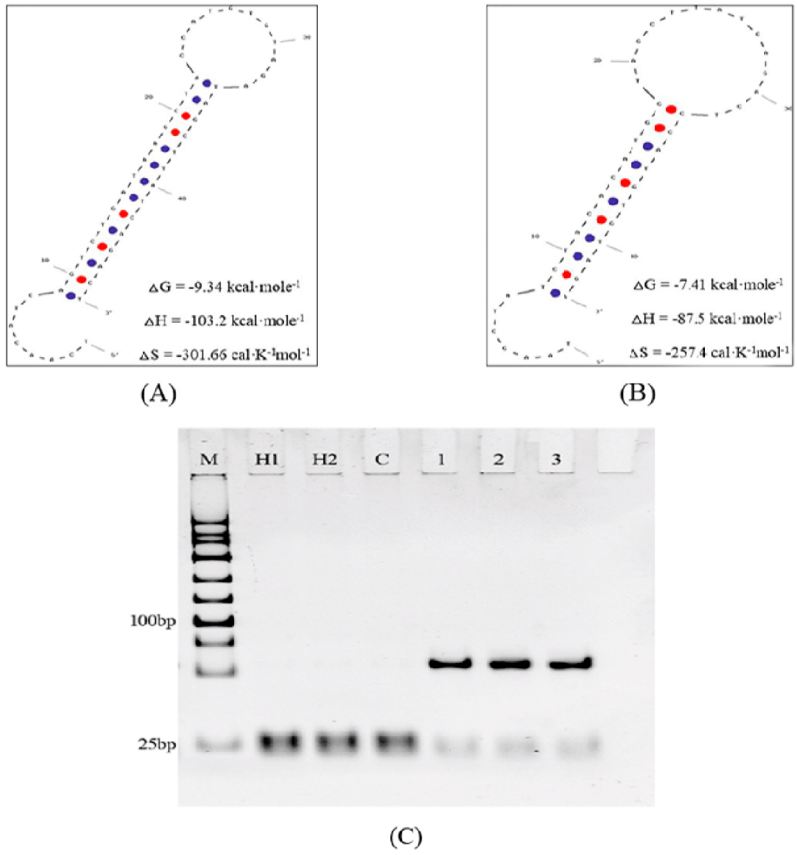

Figure 2. Ideal structure of hairpin probes and validity of the enzyme-free amplification system: (A) ideal structure and parameters of H1 probe, (B) ideal structure and parameters of H2 probe, and (C) electrophoresis of enzyme-free amplification products. The final concentration of H1 and H2 are all set as 50 nM. PBS buffer concentration is determined as 0.8×, and the RNAase inhibitor reached a concentration of 1 U/μL. Whole reactions are at 38 °C for 1 h.

On the basis of the above strategies and the sequence of miRNA21, H1 and H2 were designed. The structures were drawn in Figure 2A,B, and the parameters of hairpin probes were calculated by Oligo Analyzer 3.1. In order to verify validities of the amplification system, 10 pmol of miRNA21 was amplified by enzyme-free amplification system. The amplification products were detected by 10% polyacrylamide gel electrophoresis with the coloration of SYBR I and SYBR II. As shown in Figure 2C, the band of the 10 pmol experimental group is apparent. It indicated that the products can be stably produced from three parallel amplification experiments. Therefore, the validity of this amplification system was confirmed.

Optimizations of Experimental Parameters. After the validity of this amplification system was confirmed, we engaged in optimizations of experimental parameters. It is generally acknowledged that salt ions in solution could neutralize the charge of the nucleic acid and has a promoting effect on DNA hybridization and fabrications of hairpin structure. That means an appropriate ionic strength could bring out a strong effect on the stability of the hairpin probes' stem-and-loop structure, sensitivities, and specificities. Higher salt ionic strength could acquire a more stable hairpin-structure of H1 and H2 and plays a positive role for specificities but reduces the sensitivities to a certain extent. On the contrary, lower ionic strength gives rise to sensitivities but not specificities. For contradiction equilibriums of the ionic strength, we first explored the difference of three common buffer solutions in molecular biology, Tris-EDTA (TE) buffer, saline sodium citrate (SSC) buffer, and PBS buffer. An equivalent of miRNA21 (10 pmol) was added in the same amplification system with different buffer solutions. The signal-to-noise ratio are recorded in Figure 3A. The experimental group with PBS buffer achieves the highest signal-to-noise ratio. Thus, the PBS buffer is chosen as the reaction buffer solution. Then, we investigated the effect of PBS buffer concentration on the signal-to-noise ratio, evaluated by setting PBS concentrations as 0.2×, 0.4×, 0.6×, 0.8×, 1×, 1.2×, respectively. As shown in Figure 3B, with the increase of the PBS buffer concentration, the signal-to-noise ratio synchronously ascended. When the PBS buffer concentration was added up to 0.8×, the signal-to-noise ratio keeps at a stable level. Further addition of PBS buffer could not get a significant increase of the signal-to-noise ratio. Therefore, we employed 0.8× of GO as the optimum choice for the platform.

Temperature is an important parameter of reaction kinetics and determines the probability of collisions between the molecules. In this paper, incubating temperature is the key factor that influences the stability and interaction of the hairpins. At low temperature, H1 and H2 could not get a sufficient collision probability that greatly reduced the formation of H1−H2 complexes. Inversely, the specificity of this platform would be debased by high incubating temperature, because the temperature is interrelated with stability and integrality of hairpin probes. In the cause of incubating temperature optimization, experiments were evaluated at the temperature range from 33 to 44 °C. Experimental data was

dx.doi.org/10.1021/ac5007427 | Anal. Chem. 2014, 86, 4596−4604

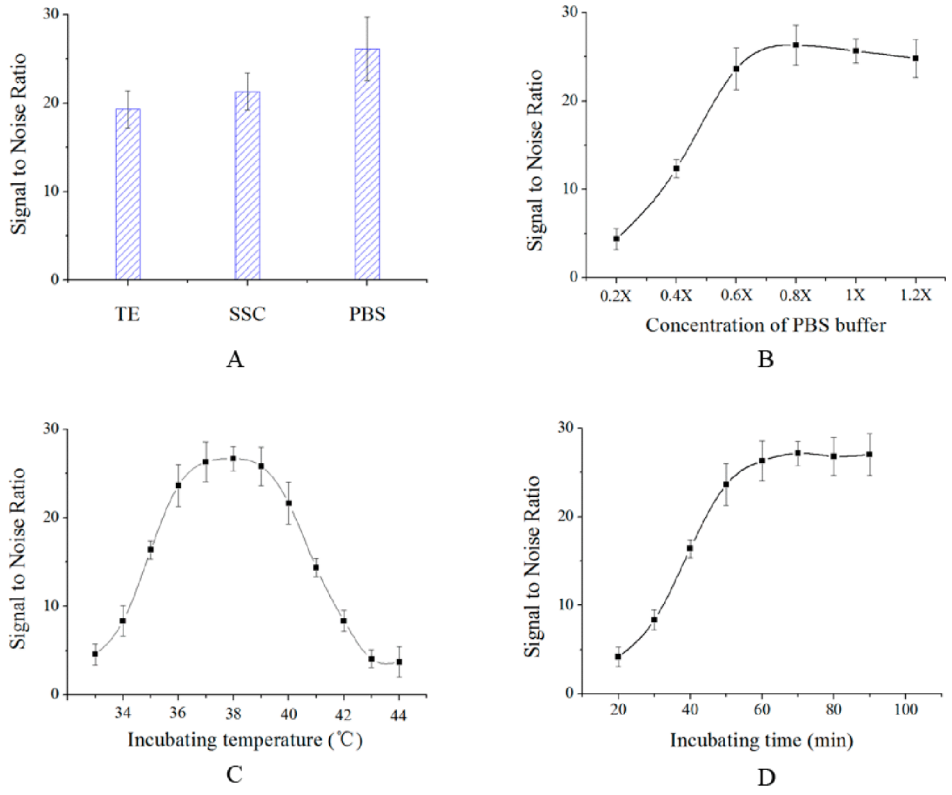

Figure 3. Optimizations of experimental parameters: (A) evaluation of the effect of buffer solutions, (B) evaluation of the effect of PBS buffer concentration on the signal-to-noise ratio, (C) evaluation of the effect of incubating temperature on the signal-to-noise ratio, and (D) evaluation of the effect of incubating time on the signal-to-noise ratio.

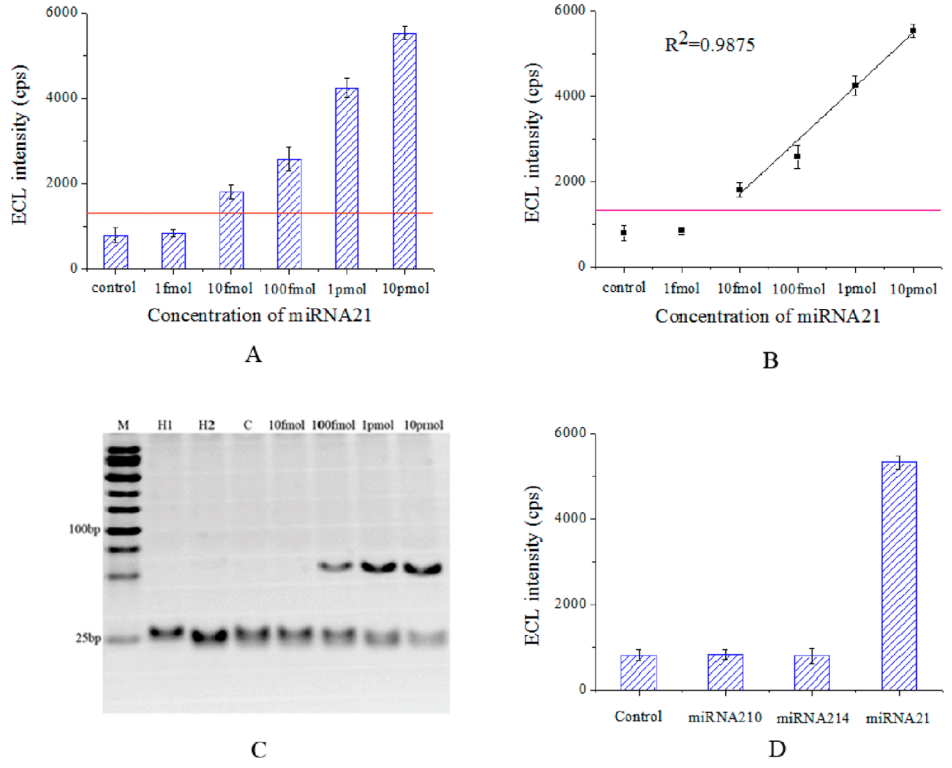

Figure 4. Sensitivity experiments for miRNA21 standard substance and specificity experiments: (A) sensitivity experiments results, (B) data analysis, and (C) electrophoresis of sensitivity experiments. The final concentration of streptavidin coated magnetic beads is 0.4 mg/mL. (D) Specificity of the enzyme-free miRNA detection platform. MiRNA210, miRNA214, and miRNA21 with an isometric concentration of 1 fM.

dx.doi.org/10.1021/ac5007427 | *Anal. Chem.* 2014, 86, 4596−4604

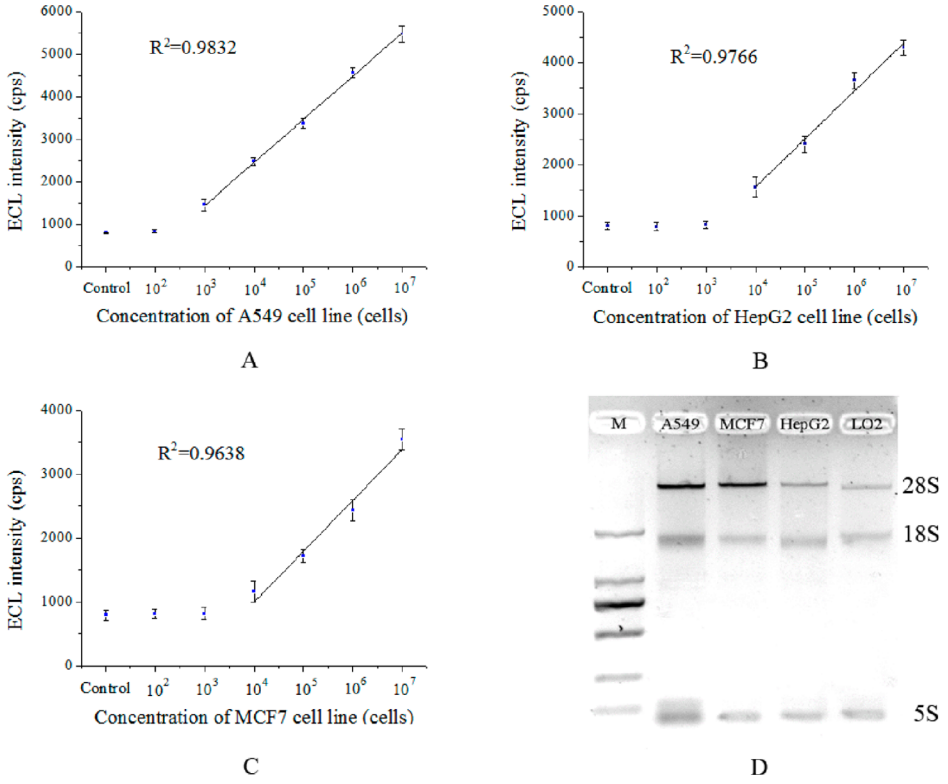

Figure 5. Sensitivity experiments for tumor cell lines and data analysis: (A) sensitivity experiments for A549 cell lines and data analysis, (B) sensitivity experiments for HepG2 cell lines and data analysis, (C) sensitivity experiments for MCF7 cell lines and data analysis, and (D) electrophoresis of total RNA extractions from tumor cell lines. All the cell lines were cultured in Dulbecco Modified Eagle Medium with 10% fetal calf serum. Before extraction, all the cell cultures were processed with cell counting.

summarized in Figure 3C and showed that we got a peak value of signal-to-noise ratio at 38 °C. Hence, 38 °C was designated as the optimum incubating temperature. In addition, incubating time is also an important parameter for this platform. For performance improvement of this platform, incubating time optimization experiments were designed by setting of the time gradient. We also employed the signal-to-noise ratio as evaluation criterion. At different incubating time point, the ECL signals were detected. The results are shown in Figure 3D. The signal-to-noise ratio ascended with the increase of incubating time. While the incubating time extended to 60 min, the signal-to-noise ratio showed a stable trend. Therefore, 60 min was chosen as the optimal incubation time.

Sensitivity and Specificity Results of the Enzyme-Free MiRNA Detection Platform. Under the optimized conditions, we executed sensitivity experiments with a different concentration of standard miRNA21 to evaluate the sensitivity of the enzyme-free miRNA detection platform. In this experiment, the concentrations of miRNA21 were varied from 1 fmol to 10 pmol. The ECL signals were observed and recorded in Figure 4A. The ECL intensity synchronously decreased with the reduction of miRNA21. When the concentration of miRNA21 depressed to 1 fmol, the ECL intensity tended to be coincident with the control group. Inversely, the group with 10 fmol of miRNA21 has an obvious enhancement compared with the control group. Through analysis, the signal-to-noise ratio of 10 fmol reached 5.704 ± 0.931 that is demonstrated that the enzyme-free miRNA detection platform achieved a high sensitivity of 10 fmol. Thus, this platform possesses high amplification efficiencies that could meet the actual demands. Then, we analyzed the linear regression analysis of the ECL intensities with a different miRNA21 concentration for verification on reliabilities of the experimental data. As shown in Figure 4B, the sensitivity results have a good linear relation from 10 fmol to 10 pmol and an R^2 value of 0.9875 was obtained. Furthermore, electrophoresis corresponding to the sensitivity experiments was executed. The results are shown in Figure 4C. Electrophoretic bands of amplification products are visible and darkened with the reduction of miRNA21 until the 100 fmol experimental group. Thus, the high amplification efficiency demonstrates that the proposed probe design strategies are effective.

Specificity is an important quality index. To further evaluate the performance of the platform, the specificity experiment was executed. In this experiment, miRNA210, miRNA214, and miRNA21 with an isometric concentration of 10 pmol were, respectively, amplified by this platform. The sequences of miRNA21, miRNA210, and miRNA214 are listed in Table. 1. Corresponding signals are obtained and shown in Figure 4D. The experimental groups of miRNA210 and miRNA214 give out a very weak ECL signal and stay at the same level of the control group. However, intense signals are observed in the miRNA21 experimental group. It is indicated that this platform has a splendid specificity that is adequate to give out a specific detection signal from the complex extractions of tumor cells and tissues.

Sensitivity Results and MiRNA21 Expression Level Comparisons of Tumor Cells. In this section, three tumor cell lines (A549, MCF-7, and HepG2) with high miRNA21 expression levels[41−44] are selected to investigate the capacities for detection of tumor cell extractions. The cell samples were processed by a total RNA extraction kit after cell counting. The

dx.doi.org/10.1021/ac5007427 | Anal. Chem. 2014, 86, 4596−4604

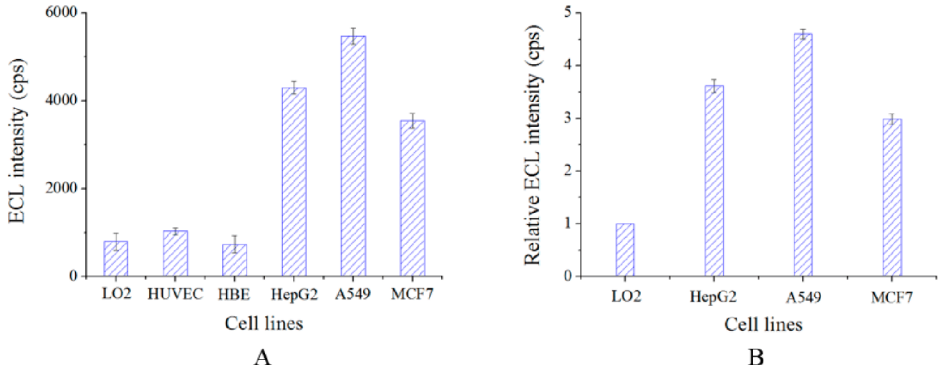

Figure 6. The miRNA21 expression difference between human normal cell lines and tumor cell lines: (A) miRNA21 expression difference between LO2, HUVEC HBE, and HepG2, A549, MCF7. (B) Comparison of miRNA21 expression level of three tumor cell lines.

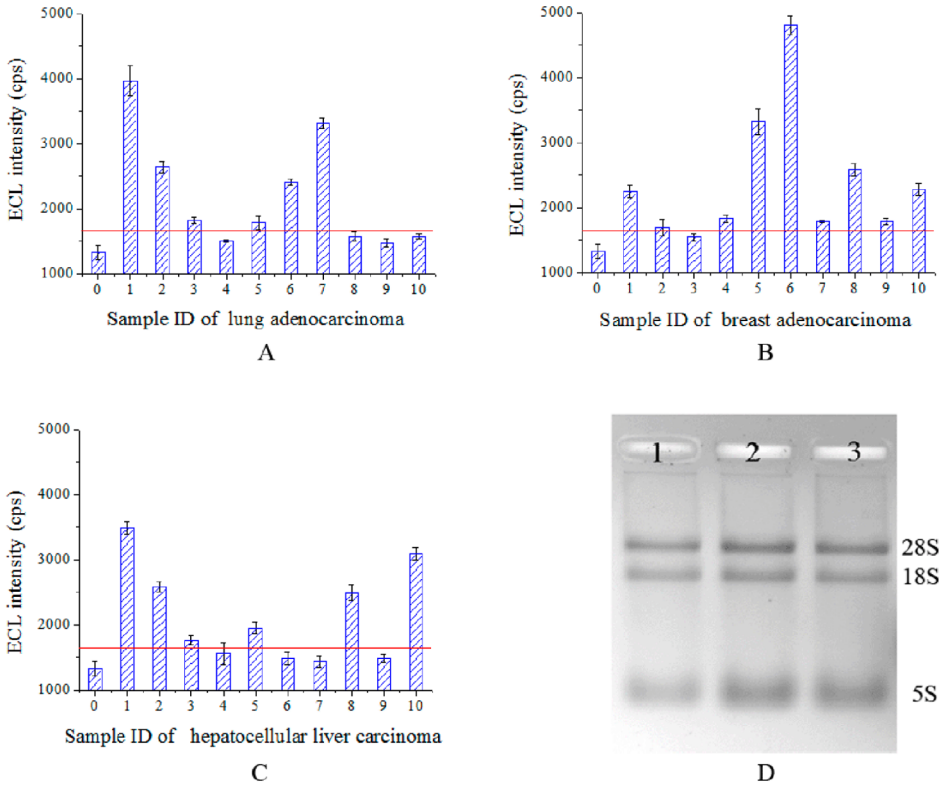

Figure 7. Tests of tumor tissues with the enzyme-free miRNA detection platform: (A) tests of human lung adenocarcinoma tissues, (B) tests of human breast adenocarcinoma tissues, (C) tests of human hepatocellular liver carcinoma tissues, and (D) electrophoresis of total RNA extractions from tumor tissues. Sample 1 is lung adenocarcinoma tissues, sample 2 is human breast adenocarcinoma tissues, and sample 3 is human hepatocellular liver carcinoma tissues. All the clinical tumor tissues were pretreated with liquid nitrogen and ground into a paste, followed by small RNA extraction by a commercial kit.

sensitivities were explored by setting the cell concentration as 10^2 cells to 10^7 cells. As shown in Figure 5A,B,C, the sensitivities of A549, HepG2, and MCF-7 reached 10^3 cells, 10^4 cells, and 10^4 cells, respectively. Through linear regression analysis of sensitivity data, the R^2 values of 0.9832, 0.9638, and 0.9766 were achieved, showed a good linear relation. Furthermore, the extractions were tested by agarose gel electrophoresis, shown in Figure 5D. Therefore, this platform possesses the capabilities for miRNA21 quantitative detection of tumor cell lines.

In addition, the difference of miRNA21 expression level between human normal cells (HUVEC, LO2, and HBE) and tumor cells (A549, MCF-7, and HepG2) is compared. RNA extractions of human normal cells and tumor cells are tested by this platform. All cell samples are set as 10^7 cells for each group. The ECL signals are recorded in Figure 6A. The ECL signals of tumor cells are obviously stronger than the human normal cells. It indicates the distinct miRNA21 expression difference between human normal cells and tumor cells. Furthermore, a comparison of miRNA21 expression levels in A549, MCF-7, and HepG2 was executed. In this section, the LO2 cell line is employed as the normal expression quantity control group of miRNA21. All cell samples are set as 10^7 cells. The ECL intensity of LO2 cell lines are artificially defined as unit 1 for intuitive characterization of miRNA21 expression levels, and the ECL intensity ratio of tumor cell lines and normal cell lines (named relative ECL intensity) is employed as the standard for miRNA21 expression levels. The results are recorded in Figure

dx.doi.org/10.1021/ac5007427 | Anal. Chem. 2014, 86, 4596−4604

6B, which indicated the different miRNA21 expression levels in three tumor cell lines.

Detection of Clinical Tumor Tissues. Clinical tumor tissues possess the complexity and diversity of features that brings great challenge to the clinical diagnosis of a tumor. Thus, an excellent tumor molecular diagnosis platform should have the capacity to cope with the complex physiological environment of tumor tissues. Here, we selected three kinds of clinical tumor tissues (corresponding to the detection assay of tumor cell lines) for further performance inspection of this platform. Three kinds of clinical tumor tissues were derived from lung adenocarcinoma, breast adenocarcinoma, and hepatocellular liver carcinoma patients. The tumor tissues were pretreated with liquid nitrogen and ground into a paste and then followed by total RNA extraction by a commercial kit. In this detection assay, 30 clinical tumor samples were tested, with each experimental group containing extractions from 1 g of tumor tissue. The experimental results were recorded in Figure 7A−C. Also, 21 of 30 experimental groups showed high expression levels of miRNA21. In addition, electrophoresis of total RNA extractions from clinical tissues is shown in Figure 7D. The electrophoresis results are consistent with the manual of total RNA extraction kit. Thus, this miRNAs detection platform possesses the potentials to be an innovation of tumor molecular diagnosis technologies. In consideration that the tumor tissues and normal tissues are intertwined, researchers could get a high accuracy via increase of sample dosages and multidraw of tumor tissues.

CONCLUSIONS

In this paper, we designed a target-triggered enzyme-free amplification platform which was realized by the circulatory interaction of target microRNA and two hairpin probes. Electrochemiluminescence (ECL) is integrated as the signal giving-out component. Benefiting from the high amplification efficiency of the enzyme-free amplification system and excellent superiority of ECL, three remarkable advantages were achieved by this platform. First, this platform operates under the condition of constant temperature. Second, the simplified reaction condition is achieved. Third, this platform reaches a high sensitivity at 10 fmol that ensured the feasibility for routine inspection and observation. Fourthly, the whole amplification process is reacted without the participation of enzyme, so inconveniences of enzyme's accretion were observably eliminated. Thus, this platform possesses potentials to be a versatile strategy for tumor molecular diagnosis and relative research.

AUTHOR INFORMATION

Corresponding Authors

*E-mail: zhouxm@scnu.edu.cn.

*E-mail: xingda@scnu.edu.cn. Phone: (+86-20) 8521-0089. Fax: (+86-20) 8521-6052.

Notes

The authors declare no competing financial interest.

ACKNOWLEDGMENTS

This research is supported by the National Basic Research Program of China (Grant 2010CB732602), the National Natural Science Foundation of China (NSFC) (Grant 81101121), the Key Program of the NSFC-Guangdong Joint Funds of China (Grant U0931005), and the Program of the Pearl River Young Talents of Science and Technology in Guangzhou, China (Grant 2013J2200021).

REFERENCES

(1) Ambros, V. *Nature* **2004**, *431*, 350−355.
(2) Cissell, K. A.; Rahimi, Y.; Shrestha, S.; Hunt, E. A.; Deo, S. K. *Anal. Chem.* **2008**, *80*, 2319−2325.
(3) Zhu, X.; Zhou, X.; Xing, D. *Chem.—Eur. J.* **2013**, *19*, 5487−94.
(4) Zhou, Y.; Huang, Q.; Gao, J.; Lu, J.; Shen, X.; Fan, C. *Nucleic Acids Res.* **2010**, *38* (15), e156.
(5) Cissell, K. A.; Shrestha, S.; Deo, S. K. *Anal. Chem.* **2007**, *79*, 4754−4761.
(6) Cho, W. C. *Mol. Cancer* **2007**, *6*, 60−67.
(7) Sedaghat-Hamedani, F.; Hassel, S.; Marquart, S.; Beier, M.; Giannitsis, E.; Hardt, S.; et al. *Clin. Chem.* **2013**, *59*, 410−418.
(8) Lee, R. C.; Feinbaum, R. L.; Ambros, V. *Cell* **1993**, *75*, 843−854.
(9) Yu, Z.; Zhu, Y.; Zhang, Y.; Li, J.; Fang, Q.; Xi, J.; Yao, B. *Talanta* **2011**, *85*, 1760−1765.
(10) Wen, Y.; Xu, Y.; Mao, X.; Wei, Y.; Song, H.; Chen, N.; Huang, Q.; Fan, C.; Li, D. *Anal. Chem.* **2012**, *84* (18), 7664−7669.
(11) Khan, N.; Cheng, J.; Pezacki, J. P.; Berezovski, M. V. *Anal. Chem.* **2011**, *83*, 6196−6201.
(12) Garzon, R.; Calin, G. A.; Croce, C. M. *Annu. Rev. Med.* **2009**, *60*, 167−179.
(13) Hwang, H. W.; Mendell, J. T. *Br. J. Cancer* **2006**, *94*, 776−780.
(14) Yue, J.; Tigyi, G. *Cancer Biol. Ther.* **2006**, *5*, 573−578.
(15) Válóczi, A.; Hornyik, C.; Varga, N.; Burgyán, J.; Kauppinen, S.; Havelda, Z. *Nucleic Acids Res.* **2004**, *32* (22), e175.
(16) Pall, G. S.; Codony-Servat, C.; Byrne, J.; Ritchie, L.; Hamilton, A. *Nucleic Acids Res.* **2007**, *35* (8), e60.
(17) Varallyay, E.; Burgyan, J.; Havelda, Z. *Nat. Protoc* **2008**, *3*, 190−196.
(18) Shi, R.; Chiang, V. L. *Biotechniques* **2005**, *39*, 519−525.
(19) Lao, K.; Xu, N. L.; Yeung, V.; Chen, C.; Livak, K. J.; Straus, N. A. *Biochem. Biophys. Res. Commun.* **2006**, *343*, 85−89.
(20) Markou, A.; Tsaroucha, E. G.; Kaklamanis, L.; Fotinou, M.; Georgoulias, V.; Lianidou, E. S. *Clin. Chem.* **2008**, *54*, 1696−1704.
(21) Chen, C. F.; Ridzon, D. A.; Broomer, A. J.; Zhou, Z. H.; Lee, D. H.; Nguyen, J. T. *Nucleic Acids Res.* **2005**, *33* (20), e179.
(22) Wang, Z.; Yang, B. *MicroRNA Expression Detect. Methods* **2010**, 131−140.
(23) Markou, A.; Tsaroucha, E. G.; Kaklamanis, L.; Fotinou, M.; Georgoulias, V.; Lianidou, E. S. *Clin. Chem.* **2008**, *54*, 1696−1704.
(24) Nelson, P. T.; Baldwin, D. A.; Scearce, L. M.; Oberholtzer, J. C.; Tobias, J. W.; Mourelatos, Z. *Nat. Meth* **2004**, *1*, 155−161.
(25) Hua, Y. J.; Tu, K.; Tang, Z. Y.; Li, Y. X.; Mao, H. S. *Genomics* **2008**, *92*, 122−128.
(26) Leung, C.-H.; Chan, D. S.-H.; He, H.-Z.; Cheng, Z.; Yang, H.; Ma, D.-L. *Nucleic Acids Res.* **2012**, *40* (3), 941−955.
(27) Goessl, C.; Krause, H.; Müller, M.; Heicappell, R.; Schrader, M.; Sachsinger, J.; Miller, K. *Cancer Res.* **2000**, *60* (21), 5941−5945.
(28) Zhu, X.; Zhou, X.; Xing, D. *Biosens. Bioelectron.* **2012**, *31* (1), 463−468.
(29) Ma, D.-L.; He, H.-Z.; Leung, K.-H.; Zhong, H.-J.; Chan, D. S.-H.; Leung, C.-H. *Chem. Soc. Rev.* **2013**, *42* (8), 3427−3440.
(30) Sardesai, N.; Kadimisetty, K.; Faria, R.; Rusling, J. *Anal. Bioanal. Chem.* **2013**, *405*, 3831−3838.
(31) Richter, M. M. *Chem. Rev.* **2004**, *104*, 3003−3036.
(32) Delaney, J. L.; Hogan, C. F.; Tian, J.; Shen, W. *Anal. Chem.* **2011**, *83*, 1300−1306.
(33) Liu, T.; Chen, X.; Hong, C.-Y.; Xu, X.-P.; Yang, H.-H. *Microchim. Acta* **2013**, 1−6.
(34) Cheng, Y.; Lei, J.; Chen, Y.; Ju, H. *Biosens. Bioelectron.* **2014**, *51* (0), 431−436.
(35) Wu, X.; Chai, Y.; Yuan, R.; Su, H.; Han, J. *Analyst* **2013**, *138* (4), 1060−1066.
(36) Miao, W. *Chem. Rev.* **2008**, *108*, 2506−2553.
(37) Yin, P.; Choi, H. M. T.; Calvert, C. R.; Pierce, N. A. *Nature* **2008**, *451*, 318−322.

(38) Li, B.; Ellington, A. D.; Xi, C. *Nucleic Acids Res.* **2011**, *39* (16), e110.
(39) Chen, X.; Briggs, N.; McLain, J. R.; Ellington, A. D. *Proc. Natl. Acad. Sci. U.S.A.* **2013**, *110* (14), 5386−5391.
(40) Jiang, Y.; Li, B.; Milligan, J. N.; Bhadra, S.; Ellington, A. D. *J. Am. Chem. Soc.* **2013**, *135* (20), 7430−7433.
(41) Wang, Z. X.; Bian, H. B.; Wang, J. R.; Cheng, Z. X.; Wang, K. M.; De, W. *J. Surg. Oncol.* **2011**, *104* (7), 847−851.
(42) Calin, G. A.; Sevignani, C.; Dumitru, C. D.; Hyslop, T.; Noch, E.; Yendamuri, S.; Shimizu, M.; Rattan, S.; Bullrich, F.; Negrini, M.; Croce, C. M. *Proc. Natl. Acad. Sci. U.S.A.* **2004**, *101* (9), 2999−3004.
(43) Iorio, M. V.; Ferracin, M.; Liu, C.-G.; Veronese, A.; Spizzo, R.; Sabbioni, S. *Cancer Res.* **2005**, *65* (16), 7065−7070.
(44) Meng, X.; Zhou, Y.; Liang, Q.; Qu, X.; Yang, Q.; Yin, H.; Ai, S. *Analyst* **2013**, *138* (12), 3409−3415.